Mechanics of Materials 102 (2016) 47–53

Contents lists available at ScienceDirect

Mechanics of Materials

journal homepage: www.elsevier.com/locate/mechmat

Effective transverse elastic properties of unidirectional fiber reinforced composites

D. Beicha[a], T. Kanit[b,*], Y. Brunet[b], A. Imad[b], A. El Moumen[c], Y. Khelfaoui[a]

[a] Laboratory of Mechanics, Materials and Energy, University of Bejaia, Algeria
[b] Laboratoire de Mécanique de Lille, Université de Lille, France
[c] Institut de Recherche Dupuy de Lome, ENSTA Bretagne, France

ARTICLE INFO

Article history:
Received 18 November 2015
Revised 19 July 2016
Available online 13 August 2016

Keywords:
Elasticity
Fiber reinforced composites
Homogenization
Hexagonal distribution
Random distribution
Microstructures

ABSTRACT

The purpose of this work was to study the influence of microstructure on effective transverse elastic behavior of fiber reinforced composites. Two microstructures were taken into account, hexagonal periodic and random arrangements of fibers. Unlike classical results at low fiber volume fractions and low Young's modulus contrast between fibers and matrices, results provided by finite elements simulations have shown that microstructure strongly affect the effective properties of composite for both high volume fractions and Young's modulus contrast. Results were compared to most common analytical models for composites elasticity.

1. Introduction

Fiber reinforced composites are known to have strength and stiffness above those of single phase materials. So they are of large interest in practical engineering situations.

First studies mainly focus on elastic behavior of aligned fibers surrounded by a matrix with the help of variational approaches. Predictive model for elasticity of such material were based on a restricted number of parameters, elasticity coefficients of each phase and fiber volume fraction, see review papers of Chamis and Sendeckyj (1968).

Until Hashin (1962), Hashin and Shtrikman (1963) and Hashin (1965), transverse microstructure of the two phases were generally not taken into account. Their models predict two bounds, between which any real microstructure could be included, especially a transverse arrangement of fibers. The lower bound, noted here HS^-, can be regarded as a disconnected arrangement of the stiffer material whereas the upper bound, HS^+, corresponds to a connected stiffer phase. Higher volume fractions were reached later with the help of the boundary element methods, see Eischen and Torquato (1993).

For simplicity, homogenization on fiber reinforced composite was usually reduced to periodic transverse distribution of fibers, see Ghosh et al. (1996) and Buryachenko (1999), while real microstructures are often random or roughly periodic with irregular boundaries.

Microstructures can be characterized statistically by different types of correlation functions, see Torquato (1998). For simplicity, we restrain microstructure description to two-point correlation function, even if at short distances it does not allow a fine description of periodic materials. For mono-disparity in size of non-overlapping fibers, the easier two-point correlation function is the pair distribution function of Hansen and McDonald (1987), which only refers to the positions of fiber centers r_i in the transverse section:

$$g(r) = \frac{1}{\rho N} \sum_{i} \sum_{j \neq i} \delta\left(r - r_{ij}\right) \tag{1}$$

In which $\rho = N/S$ is the number N of fibers per unit transverse surface S of the specimen and r the dimensionless space coordinate. Such as $|r|$ is just equal to 1 at contact between fibers. A physical interpretation of $g(r)$ is the number of fiber centers located in a volume dr at a distance r from a test fiber, divided by the number of fibers given by a uniformly distributed fiber field.

Hexagonal periodic composites were not isotropic and exhibit 6 preferred directions related to the 6 near neighbors of the test fiber. For a mathematically perfect periodic specimen, $g(r)$ cannot be represented by a function. It is a spatial distribution of Dirac distributions but in practice, there is always an uncertainty on fiber locations. The hexagonal morphology suggests expressing r in cylindrical coordinates(r, θ). An inclusion located at (r, θ) from

* Corresponding author.
E-mail address: toufik.kanit@univ-lille1.fr (T. Kanit).

http://dx.doi.org/10.1016/j.mechmat.2016.08.010

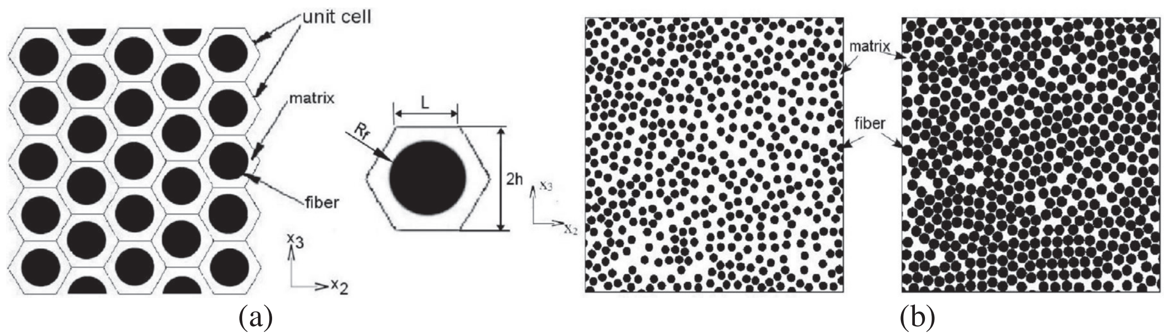

Fig. 1. Morphology of microstructures, (a) hexagonal arrangement and unit periodic cell in the transverse plane and (b) random distribution with volume fraction $P = 0.4 = 40\%$ at left and $P = 0.65$ at right.

the test inclusion is in reality placed in a bin of sizes $r\delta r\delta\theta$. At short distance r, the number of fibers in a bin is very sensitive to θ, whereas at long distance it becomes independent or quasi isotopic as it was for a random composite. As $g(r)$ is characteristic of long range interactions one could expect a similar effective elastic behavior for random and hexagonal composites.

Actually at same volume fraction and elasticity contrast between phases, hexagonal and random composites were expected to have rather similar behavior because their microstructures become alike at long distance. It was effectively still observed at low fiber density and weak elasticity contrast, see Trias et al. (2006). But for high volume fraction and high elasticity contrast, there is still a doubt that microstructure influences effective elasticity of composites.

Present work is a comparison between effective elastic properties of fiber reinforced composite respectively built with hexagonal and random distribution of non overlapping fibers, for a large range of volume fraction P of fibers and elasticity contrast c. The homogenized effective transverse elastic properties of these composites were provided by finite element simulations followed by a volume averaging of local properties. Results will be compared to few analytical constitutive equations for elasticity of composite provided by Hashin (1962), Hashin and Shtrikman (1963), Christensen and Lo (1979) and Hervé and Zaoui (1995).

2. Morphology description and finite element meshes

2.1. Microstructure generating

The composite under consideration were all reinforced with cylindrical fibers of same diameters. Apart from volume fraction and elasticity contrast, the only difference between samples studied was the fiber transverse distribution which could be distributed randomly or periodically along a hexagonal frame.

Determination of homogenized effective transverse elastic properties of these composites requires samples large enough to reach a representative elementary volume (RVE) and so to ensure statistical homogeneity. Due to its periodicity, the RVE in hexagonal situation is reduced to a hexagonal cell surrounding a single fiber. The unit cell is characterized by L and h dimensions and by the radius R_f of fiber with an associated frame of reference where the transverse plane is (x_2x_3)as shown on Fig. 1.

For random samples, the RVEs have to ensure that the apparent overall elasticity moduli were independent of the boundary conditions. According to Hill (1963), the RVE must contains a sufficient number of fibers and as it was pointed out by Kanit et al. (2003), it must have a sufficiently large size with regard to fiber diameters. For higher volume fractions, 500 fibers were insufficient to capture the localized behavior and the associated boundary layer had a noticeable effect. An ensemble averaging on 10 differents samples was necessary to reach convergence of the overall elasticity moduli. Examples of random samples are sketched on Fig. 1.

For hexagonal samples, the range of fiber volume fraction was from $P = 0$ to critical volume fraction $P_{crit} = \sqrt{3}\pi/2 = 0.907$ that corresponds to $h = R_f$, whereas for random samples volume fracton did not exceed the jamming limit $P = 0.65$.

2.2. Meshing

Except for the hexagonal cell, meshes were provided by superposition of finite elements square grids on microstructure images using multi-phase elements technique. Then elastic properties of the phases were associated to each integration point. This technique initially developed by Lippmann et al. (1997) was then used by El Moumen et al. (2013) and El Moumen et al. (2014). For hexagonal unit cells, an example of used mesh is presented on Fig. 2 as well as its deformation under a simple shear.

In order to ensure accurate results, even in high stress gradients situations, the finite element mesh must be fine enough to avoid dependence of results with mesh scales. Different meshes were tested with regard to mesh densities. Fig. 3 presents results of convergence for random and hexagonal samples with volume fraction $P = 0.51$.

Of course the convergence was easier for the hexagonal configuration in which a RVE is reduced to a single cell. In both configurations the final mesh was fined enough to represent accurately the geometry of inclusions.

2.3. Linear elasticity and applied strain

For transverse isotropic problems, in the case of two phases, fibers f in a matrix m, the plane bulk modulus k_m and k_f and the plane shear modulus μ_m and μ_f of the matrix and fibers are related to the Young's moduli E_m and E_f and Poisson's ratios ν_m and ν_f as follows,

$$k_i = \frac{E_i}{2(1+\nu_i)(1-2\nu_i)}, \mu_i = \frac{E_i}{2(1+\nu_i)}, i = m, f \quad (2)$$

Both transverse effective bulk k^* and shear μ^* moduli were calculated by solving two fundamental boundary value problems with imposed strain. The macroscopic imposed strain tensors $\tilde{E}$ were given respectively by:

$$\tilde{E}^k = \begin{pmatrix} 1 & 0 \\ 0 & 1 \end{pmatrix} \text{and } \tilde{E}^\mu = \begin{pmatrix} 0 & \frac{1}{2} \\ \frac{1}{2} & 0 \end{pmatrix} \quad (3)$$

Then macroscopic plane bulk modulus k^* and shear modulus μ^* are computed as:

$$k^* = \langle\tilde{\sigma}\rangle : \tilde{E}^k = \frac{1}{4}[trace(<\sigma>)] \text{and } \mu^* = \langle\tilde{\sigma}\rangle : \tilde{E}^\mu = \langle\sigma_{12}\rangle \quad (4)$$